

**Modelling coupled water and heat transport in a soil-mulch-plant-atmosphere continuum (SMPAC) system**

**C.L. Wu<sup>1</sup>, K.W. Chau<sup>\*2</sup> and J.S. Huang<sup>3</sup>**

<sup>1</sup>*Changjiang Water Resources Commission, 430010, Wuhan, People's Republic of China*

<sup>2\*</sup>*Department of Civil and Structural Engineering, Hong Kong Polytechnic University, Hung Hom, Kowloon, Hong Kong, People's Republic of China. (Email: cekwchau@polyu.edu.hk)*

<sup>3</sup>*Department of Civil and Environmental Engineering, Wuhan University, 430072, Wuhan, People's Republic of China*

**Abstract**

This paper presents a physically based model coupling water and heat transport in a soil-mulch-plant-atmosphere continuum (SMPAC) system, in which a transparent polyethylene mulch is applied to a winter wheat crop. The purpose of the study is to simulate profiles of soil water content and temperature for different stages of wheat growth. The mass and energy balance equations are constructed to determine upper boundary conditions of governing equations. Energy parameters are empirically formulated and calibrated from three-month field observed data. Resistance parameters in the SMPAC system are calculated. The mass and energy equations are solved by an iterative Newton-Raphson technique and a finite difference method is used to solve the governing equations. Water-consuming experiments are performed within the growing period of wheat. The results show that the model is quite satisfactory, particularly for high soil water content, in simulating the water and temperature profiles during the growth of the winter wheat.

*Keywords:* Transparent polyethylene mulch; SMPAC system; Energy balance equations; Coupled water and heat transport model.

**1. Introduction**

The transparent polyethylene mulch is used, particularly in arid (or semiarid) and frigid regions, for conserving soil temperature and water content to improve crop growth (Mahrer et al., 1984; Flerchinger et al., 2003). The formation of water droplets on the inner surface of the polyethylene film highly reduces transmissivity of long-wave radiation but does not affect short-wave radiation, which in turn reduces heat convection and evaporation from the soil. The cropland with mulch is a very complicated system because the covering influences the soil surface radiation balance, the soil water evaporation rate, and the soil temperature and moisture distribution.

Several soil-mulch-atmosphere continuum (SMAC) studies have been developed to investigate the effects of various soil-surface coverings on the temperature and water distribution in the soil. Mahrer et al. (1984) studied the heat and water flow with a transparent polyethylene mulch covering the entire surface. Chung and Horton (1987) employed a finite difference method to simulate the coupled soil water and heat flow with a partial surface mulch. Ham and Kluitenberg (1994) investigated the effect of mulch optical properties and mulch-soil contact resistance on soil heating. Flerchinger et al. (2003) modeled effects of crop residue cover and architecture on heat and water transfer at the soil surface. Findeling et al. (2003a) developed a model for water and heat flows through a mulch allowing for radiative and long-distance convective exchanges in the mulch. However, the plant (or canopy) is not taken into account in all the above-mentioned studies.

For the cases without a mulch, soil-plant-atmosphere continuum (SPAC) systems have been

---

\* corresponding author

studied by various researchers. The plant varied from crop, such as cereal (Kim et al., 1989), maize (McGinn and King, 1990), lettuce (Luo et al., 1992), and wheat (Alves et al., 1998), to forests (Lafleur, 1992). Most of these studies focused on the energy distribution and evapotranspiration in the system. However, neither the SMAC nor the SPAC systems can mimic the real situation completely. The energy in the system will be redistributed considerably and more parameters are involved when a mulch layer is incorporated into the SPAC system or when the plant is considered in the SMAC system. Huang and Shen (1999) constructed a soil-mulch-plant-atmosphere continuum (SMPAC) system to estimate crop evapotranspiration. Findeling et al (2003b) and Gonzalez-Sosa et al. (1999 & 2001) studied the effects of a partial residue mulch on runoff using a physically based approach. However, in their models, many parameters were very simplified.

In the present study, a four-layered SMPAC model is developed to simulate water and heat transport in a wheat cropland covered by transparent polyethylene. Empirical parameters are determined from three-month field measurements. Soil surface boundary conditions are derived from energy balance equations. The key objective of this paper is to simulate the soil water and heat transport mechanisms in the SMPAC system under different growing phases of the wheat, which will be useful for irrigation purposes.

## 2. Materials and Methods

### 2.1 Description of the model

#### 2.1.1 System schematization

Fig.1 shows a schematic diagram of this system, which is divided into four layers: an atmosphere layer at reference height; a plant layer at the height of momentum transfer confluence based on the big leaf model (Alves et al., 1998); a transparent polyethylene layer covering on the topsoil of the cropland; and a soil layer, with a bottom boundary at a depth of 100cm. Values of soil water content and temperature in the soil come from field observation. Several assumptions are made on the plant layer at this point. The plant layer is uniform and horizontal. The transfer amount from molecular diffusion is negligible comparing with that from turbulent diffusion due to the wind speed under the experimental conditions. The net radiation absorbed by the plant canopy is entirely used for exchange in the form of sensible heat and latent heat with the surrounding air. Moreover, the transfer fluxes of sensible heat and latent heat in the vertical direction are formulated by the gradient-diffusion theory.

#### 2.1.2 Governing equations

The governing equations of water and heat flow in the soil are based on mass conservation and energy conservation, respectively. Since water contents of studied soil will vary from saturation water content to residual water content, the non-isothermal coupled equations are adopted here (Milly, 1984). Moreover, the plant transpiration flux is incorporated into mass conservation equation in the form of absorption rate of the root to reflect the growth of wheat.

The governing equations are written as:

$$G_h \frac{\partial h}{\partial t} + G_T \frac{\partial T}{\partial t} = \frac{\partial}{\partial z} [D_{Tv} \frac{\partial T}{\partial z}] + \frac{\partial}{\partial z} [K + D_{hv}] \frac{\partial h}{\partial z} - \frac{\partial K}{\partial z} - S_r \quad (1)$$

$$S_T \frac{\partial T}{\partial t} + S_h \frac{\partial h}{\partial t} = \frac{\partial}{\partial z} [(\lambda + L_m \rho_l D_{Tv}) \frac{\partial T}{\partial z}] + \frac{\partial}{\partial z} [L_m \rho_l D_{hv}] \frac{\partial h}{\partial z} - \frac{\partial}{\partial z} [c_l (T - T_0) q_l] \quad (2)$$

with the corresponding coefficients as follows

$$G_h = [(1 - \frac{\rho_v}{\rho_l}) (\frac{\partial \theta_l}{\partial h})_T + \frac{\theta_v}{\rho_l} (\frac{\partial \rho_v}{\partial h})_T] \quad (3)$$

$$G_T = [(1 - \frac{\rho_v}{\rho_l}) (\frac{\partial \theta_l}{\partial T})_h + \frac{\theta_v}{\rho_l} (\frac{\partial \rho_v}{\partial T})_h] \quad (4)$$

$$S_T = C + H_2 \frac{\partial \theta_l}{\partial T} + H_1 \theta_v \frac{\partial \rho_v}{\partial T} \quad (5)$$

$$S_h = H_2 \frac{\partial \theta_l}{\partial h} + H_1 \theta_v \frac{\partial \rho_v}{\partial h} \quad (6)$$

where  $C = c_s \rho_s (1 - n) + c_l \rho_l \theta_l + c_v \rho_v \theta_v$ ,  $H_1 = L_0 + c_p (T - T_0)$ , and

$H_2 = (c_l \rho_l - c_p \rho_v)(T - T_0) - L_0 \rho_v$ ;  $\rho_l$  is the density of liquid water ( $\text{kg m}^{-3}$ );  $\rho_s$  is the density of solid part of the soil ( $\text{kg m}^{-3}$ );  $K$  is the hydraulic conductivity ( $\text{ms}^{-1}$ );  $h$  is the matric potential (m);  $z$  is the vertical space coordinate with positive downward direction (m);  $q_l$  is the liquid flux ( $\text{kg m}^{-2} \text{s}^{-1}$ );  $\theta_l$  is the volumetric liquid water content ( $\text{m}^3 \text{m}^{-3}$ );  $\theta_v$  is the volumetric air content ( $\text{m}^3 \text{m}^{-3}$ );  $\theta_v = n - \theta_l$ ;  $n$  is the porosity of the soil;  $\rho_v$  is the absolute humidity of soil air ( $\text{kg m}^{-3}$ ), and  $\rho_v(h, T) = \rho_0(T) \exp(hg / R(T + 273.16))$ ;  $\rho_0$  is the saturation vapor density ( $\text{kg m}^{-3}$ );  $g$  is the gravitational acceleration ( $\text{m s}^{-2}$ );  $R$  is the gas constant for water vapor ( $461.5 \text{ m}^2 \text{s}^{-2} \text{K}^{-1}$ );  $T$  is the temperature in degrees Celsius ( $^{\circ}\text{C}$ );  $C$  is the volumetric heat capacity of the soil ( $\text{J m}^{-3} \text{ }^{\circ}\text{C}^{-1}$ );  $c_l$  is the mass heat capacity of liquid water ( $\text{J kg}^{-1} \text{ }^{\circ}\text{C}^{-1}$ );  $c_v$  is the mass heat capacity of water vapor ( $\text{J kg}^{-1} \text{ }^{\circ}\text{C}^{-1}$ );  $c_p$  is the mass heat capacity of water vapor at constant pressure ( $\text{J kg}^{-1} \text{ }^{\circ}\text{C}^{-1}$ );  $\lambda$  is the effective thermal conductivity ( $\text{J s}^{-1} \text{ m}^{-1} \text{ }^{\circ}\text{C}^{-1}$ );  $T_0$  is the temperature datum for zero enthalpy ( $^{\circ}\text{C}$ );  $L_m$  is the mass latent heat of vaporization of water ( $\text{J kg}^{-1}$ ) and

$L_m = L_0 - (c_l - c_p)(T - T_0)$ ;  $L_0$  is the value of  $L_m$  evaluated at the temperature  $T_0$ ;  $S_r$  is the water absorption rate of the plant root ( $\text{s}^{-1}$ );  $D_{hv}$  is the vapor conductivity ( $\text{m s}^{-1}$ ); and,  $D_{Tv}$  is the thermal vapor diffusion coefficient ( $\text{m}^2 \text{s}^{-1} \text{ }^{\circ}\text{C}^{-1}$ ).

### 2.1.3 Energy balance equation

Soil surface temperature and evaporation rate are determined implicitly from the surface energy balance in the SMPAC system. With reference to Fig. 1, the energy balance equations for the atmosphere layer, plant layer, transparent polyethylene layer, and soil layer are described respectively as follows:

$$R_n - H_{pa} - LE - G = 0 \quad (7)$$

$$(\alpha_{pg} + r_{mg} t_{pg}) R_g + (\alpha_{pl} + r_{ml} t_{pl}) R_l + (r_{ml} - 2) \varepsilon_p \sigma T_p^4 + \varepsilon_m \sigma T_m^4 + t_{ml} \varepsilon_s \sigma T_s^4 + H_{mp} - LE - H_{pa} = 0 \quad (8)$$

$$(\alpha_{mg} + r_{sg} t_{mg}) t_{pg} R_g + \alpha_{ml} (t_{pl} R_l + \varepsilon_p \sigma T_p^4) - 2 \varepsilon_m \sigma T_m^4 + \alpha_{ml} \varepsilon_s \sigma T_s^4 + H_{sm} - H_{mp} = 0 \quad (9)$$

$$(1 - r_{sg}) t_{mg} t_{pg} R_g + t_{ml} (t_{pl} R_l + \varepsilon_p \sigma T_p^4) + \varepsilon_m \sigma T_m^4 - (1 - r_{ml}) \varepsilon_s \sigma T_s^4 - H_{sm} - G = 0 \quad (10)$$

where  $R_n$  is net radiation ( $\text{W m}^{-2}$ ) (positive downward);  $H_{pa}$  is sensible heat transfer flux from the plant layer to atmosphere layer ( $\text{W m}^{-2}$ );  $H_{lp}$  is sensible heat transfer flux from leaves of plant to the plant layer ( $\text{W m}^{-2}$ );  $H_{mp}$  is sensible heat transfer flux from mulch layer to the plant layer ( $\text{W m}^{-2}$ );  $H_{sm}$  is sensible heat transfer flux from soil layer to mulch layer ( $\text{W m}^{-2}$ );  $L$  is the volumetric latent heat of vaporization ( $\text{J m}^{-3}$ );  $E$  is the evaporative flux ( $\text{m s}^{-1}$ );  $LE$  is potential latent heat transfer flux from the plant layer to atmosphere layer ( $\text{W m}^{-2}$ ) (positive upward);  $R_g$  is the measured global radiation ( $\text{W m}^{-2}$ );  $R_l$  is the long-wave sky irradiance ( $\text{W m}^{-2}$ );  $T_a$  is air temperature ( $^{\circ}\text{C}$ );  $T_p$  is temperature of the plant layer surface ( $^{\circ}\text{C}$ );  $T_m$  is temperature of the mulch surface ( $^{\circ}\text{C}$ );  $T_s$  is soil surface temperature ( $^{\circ}\text{C}$ );  $\alpha_{pg}$  is absorptivity for global radiation of the plant layer;  $\alpha_{pl}$  is absorptivity for the long-wave sky irradiance of the plant layer;  $\alpha_{mg}$  is

mulch absorptivity for global radiation;  $\alpha_{ml}$  is mulch absorptivity for the long-wave sky irradiance;  $r_{ml}$  is mulch surface albedo for the long-wave sky irradiance;  $r_{mg}$  is mulch surface albedo for global radiation;  $r_{sg}$  is soil surface albedo for global radiation;  $r_{pg}$  is surface albedo for global radiation of the plant layer;  $t_{pg}$  is transmissivity for global radiation of the plant layer;  $t_{pl}$  is transmissivity for the long-wave sky irradiance of the plant layer;  $t_{mg}$  is mulch transmissivity for global radiation;  $t_{ml}$  is mulch transmissivity for the long-wave sky irradiance;  $\sigma$  is the Stefan-Boltzmann constant ( $5.67 \times 10^{-8} \text{ W m}^{-2} \text{ K}^{-4}$ );  $\varepsilon_p$ ,  $\varepsilon_m$ , and  $\varepsilon_s$  are the emissivity of the plant layer, mulch, and soil, respectively; and,  $G$  is the soil heat flux at the soil surface ( $\text{W m}^{-2}$ ) (positive downward). In the formulation, reflections of second order or more, as well as long-wave reflection of mulch thermal radiation on the plant and the soil, are neglected.

The net radiation  $R_n$  is calculated as:

$$R_n = R_s + (1 - r_{pl})R_l - \varepsilon_p \sigma T_p^4 \quad (11)$$

where  $R_s$  is the short-wave sky irradiance ( $\text{W m}^{-2}$ ), which is expressed as:

$$R_s = (1 - \gamma_{pg})R_g \quad (12)$$

while  $R_l$  is expressed as (Van Bavel and Hillel, 1976):

$$R_l = \sigma (T_a + 273.16)^4 [0.605 + 0.048(1370H_a)^{1/2}] \quad (13)$$

where  $H_a$  is the air absolute humidity ( $\text{kg m}^{-3}$ ).

The soil heat flux  $G$  is written as:

$$G = \lambda \frac{\partial T}{\partial z} \quad (14)$$

Based on the assumption of gradient-diffusion theory, the fluxes of sensible heat and latent heat between different layers in the SMPAC system are computed by:

$$H_{pa} = \rho_a c_p (T_p - T_a) / r_a^a \quad (15)$$

$$H_{lp} = \rho_a c_p (T_l - T_p) / r_a^c \quad (16)$$

$$H_{mp} = \rho_a c_p (T_m - T_p) / r_m^p \quad (17)$$

$$H_{sm} = \rho_a c_p (T_s - T_m) / r_s^m \quad (18)$$

$$LE = \frac{\rho_a c_p}{\gamma} \frac{e_p - e_a}{r_a^a} \quad (19)$$

$$LE_p = \frac{\rho_a c_p}{\gamma} \frac{e_{sat}(T_l) - e_p}{r_a^p + r_a^c} \quad (20)$$

where  $\rho_a$  is the density of air ( $\text{kg m}^{-3}$ );  $\gamma$  is the psychrometric constant ( $\text{mba } ^\circ\text{C}^{-1}$ );  $LE_p$  is total potential latent heat transfer flux within canopy ( $\text{W m}^{-2}$ ) whose transfer occurs between stomatal cavities of leaves and the momentum confluence location;  $e_a$  is air vapor pressure at reference height (mba);  $e_p$  is air vapor pressure at the momentum confluence location (mba);  $e_{sat}(T_l)$  is the saturated vapor pressure within stomatal cavities of leaves at temperature  $T_l$  (mba);  $T_l$  is leaf temperature ( $^\circ\text{C}$ );  $r_a^a$  is the resistance to convective heat transfer or vapor transfer between atmosphere layer and ambient air within the plant layer ( $\text{s m}^{-1}$ );  $r_a^c$  is the aerodynamic boundary layer resistance within the plant layer ( $\text{s m}^{-1}$ );  $r_a^p$  is the stomatal resistance of all leaves ( $\text{s m}^{-1}$ );  $r_m^p$  is the resistance to convective heat transfer from the mulch layer to the plant layer ( $\text{s m}^{-1}$ ); and,

$r_s^m$  is the resistance to convective heat transfer between the soil surface and mulch layer ( $s\ m^{-1}$ ).

Owing to the complete surface mulch with transparent polyethylene, it is assumed that no latent heat transfer takes place between soil layer, mulch layer, and the plant layer. Thus, evaporation does not occur and only transpiration from the plant layer takes place. In the transpiration process, water enters from the soil, through roots, xylems, to stomatal cavities of leaves, and finally transpires in form of vapor to the ambient air in the plant layer.

## 2.2 Description of the experiment

### 2.2.1 The cropland

The cropland is a semiarid region located at the suburb of Beijing. Its yearly precipitation is about 600mm, though mostly concentrated in summer. The growth period of wheat is generally from November to June in the next year. In the experiment, six plots are employed, and each plot is with an extent of length 15 m and width 12 m. And, each plot consists of six ribbings. Four out of six plots are considered for the mulch experiment. During the experiment, each ribbing of the plot is covered with transparent polyethylene after wheat seeds have been sown. When seedlings come out of soil, the transparent polyethylene is lacerated to let them pass through the mulch.

### 2.2.2 Measurements

The field tests are carried out from March 15 to June 10, 2003 when the wheat is harvested. In each plot, the temperatures of mulch surface, surface soil, and soil profile and the water content of soil profile are measured. It is three times per day about the temperature measurement of mulch surface and surface soil. i.e. 8.00 am, 2.00 pm, and 8.00pm. The temperature of soil profile and the water content of soil profile are generally measured one time per 5 days. The water content profile will be measured when it rains in some day. The depth profiles for measuring soil temperature and water content are at 0, 10, 20, 30, 40, 60, 100cm and 0, 10, 20, 30, 40, 60, 80, 100cm, respectively. The texture of soil at depth ranging from 0 to 70cm is silt loam whilst that below 70cm is sand.

Other parameters, such as wind velocity at the reference height, atmosphere pressure, water vapor pressure and so on, are obtained from the micro-meteorological station near the cropland.

## 2.3 Determination of model parameters and input variables

### 2.3.1 Initial and boundary conditions

The initial conditions of temperature and matric potential at each discretization node in the study area at the beginning of the simulation are expressed as follows:

$$h(z, t)|_{t=0} = h(z, 0) \quad 0 \leq z \leq 100cm \quad (21)$$

$$T(z, t)|_{t=0} = T(z, 0) \quad 0 \leq z \leq 100cm \quad (22)$$

where  $z$  is depth of the soil (cm).  $h(z, 0)$  and  $T(z, 0)$  are obtained by field observation whilst values at the nodes without field data are obtained by linear interpolation method.

The top boundary conditions are Neumann conditions, namely the total mass flux of water (water and vapor) and the total heat flux (sensible and latent heat) whilst the bottom boundary conditions are Dirichlet conditions of matric potential and temperature. The bottom boundary conditions are described as follows:

$$h(z, t)|_{z=100} = h(100, t) \quad t \geq 0 \quad (23)$$

$$T(z, t)|_{z=100} = T(100, t) \quad t \geq 0 \quad (24)$$

During the growth period of the wheat, matric potentials and temperatures of soil profile are observed with an interval of 5 days and, in addition, when precipitation occurs. Quadratic curve fitting is employed to obtain daily bottom boundary conditions for the simulation. The heat flux  $G$  is determined from the soil surface temperature  $T_s$  via the solution to energy balance equations. The flux of moisture in the soil is expressed as:

$$q_m \Big|_{z=0} = -[(K + D_{hv}) \frac{\partial h}{\partial z} + D_{Tv} \frac{\partial T}{\partial z} - K] \Big|_{z=0} \quad (25)$$

where  $q_m$  is the total mass flux of water.  $G$  and  $q_m$  act as sink/source terms in the determination of the appropriate boundary conditions. Moreover, measured rainfall and runoff records are used to correlate with the boundary conditions.

### 2.3.2 Soil, mulch and plant properties

#### 2.3.2.1 Volumetric soil water content $\theta_l$

The relationship between the soil water content and pressure head proposed by Van Genuchten (1980) is adopted as follows:

$$\theta_l = \theta_r + \frac{(\theta_s - \theta_r)}{[1 + (\alpha |h|)^n]^m} \quad (26)$$

where,  $\theta_s$  and  $\theta_r$  are saturated and residual values of the soil water content ( $\text{m}^3 \text{m}^{-3}$ ), respectively;  $m$  and  $n$  are shape parameters following the relationship  $m = 1 - 1/n$  and  $\alpha$  ( $\text{m}^{-1}$ ) is a scaling parameter of the matric potential. According to the estimation from observed soil water retention data in the laboratory test (i.e. the suction table), the estimated values for  $\theta_s$ ,  $\theta_r$ ,  $\alpha$ , and  $n$  are obtained as shown in Table 1.

#### 2.3.2.2 Soil hydraulic conductivity $K$ and soil thermal conductivity $\lambda$

The hydraulic conductivity  $K$  is expressed as an empirical function of matric potential  $h$  Chung and Horton (1987):

$$K(h) = P |h|^Q \quad (27)$$

where  $P$  and  $Q$  are the regression parameters. An empirical formulation employed by Chung and Horton (1987) is adopted for the thermal conductivity  $\lambda$  in terms of volumetric water content  $\theta_l$ :

$$\lambda(\theta_l) = b_1 + b_2 \theta_l + b_3 \theta_l^{0.5} \quad (28)$$

where  $b_1$ ,  $b_2$  and  $b_3$  are the regression parameters according to the established relationship between  $\lambda$  and  $\theta_l$ . The observed data used to carry out the regressions are soil thermal conductivity and pressure head. Parameters  $P$ ,  $Q$ ,  $b_1$ ,  $b_2$  and  $b_3$  are obtained as detailed in the model calibration below.

#### 2.3.2.3 Volumetric soil heat capacity $C$

The volumetric soil heat capacity is a weighted average of the capacities of its components:

$$C = c_s \rho_s (1 - n) + c_l \rho_l \theta_l + c_v \rho_v \theta_v \quad (29)$$

#### 2.3.2.4 Vapor conductivity $D_{hv}$ and thermal vapor diffusion coefficient $D_{Tv}$

The vapor conductivity  $D_{hv}$  is formulated as follows (Milly and Eagleson, 1980):

$$D_{kv} = \rho_l^{-1} D_a \Omega \theta_v \rho_v g / (R(T + 273.16)) \quad (30)$$

where  $D_a$  is the molecular diffusivity of water vapor in air ( $\text{m}^2 \text{s}^{-1}$ )

$$D_a = 2.29 \times 10^{-5} \left(1 + \frac{T}{273.16}\right)^{1.75} \quad (31)$$

and parameter  $\Omega$  represents the tortuosity of the air-filled pore domain, which is expressed as:

$$\Omega = (n - \theta_l)^{2/3} \quad (32)$$

The diffusion coefficient for vapor transport due to temperature gradients  $D_{Tv}$  is expressed as (de Vires, 1958):

$$D_{Tv} = \rho_l^{-1} f D_a \theta_v \rho_v (4975.9 - hg/R)/(T + 273.16)^2 \quad (33)$$

$$\text{where } \begin{cases} f = n & \theta_l \leq \theta_{lk} \\ f = \theta_a + \frac{\theta_a \theta_l}{(n - \theta_{lk})} & \theta_l > \theta_{lk} \end{cases} \quad (34)$$

in which  $\theta_{lk}$  is the critical value of  $\theta_l$  for hydraulic connectivity.

Water absorption rate of root  $S_r(z, t)$

The water absorption rate of root  $S_r(z, t)$  is formulated as follows (Bolger et al., 1992):

$$S_r(z, t) = \frac{A}{d(t)} T_r(t) \bullet \exp(-B(\frac{z}{d(t)} - C)^2) \quad (35)$$

where  $T_r(t)$  is the transpiration rate of wheat at time  $t$  ( $\text{m s}^{-1}$ );  $d(t)$  is the root depth into soil at time  $t$  along  $z$  coordinates (cm);  $A$ ,  $B$ , and  $C$  are the fitting coefficients, with values of 0.13812, 2.6818, and 0.27032 respectively in this study based on the relationship between root density ( $\text{g cm}^{-3}$ ) and soil depth (m) by employing the least square method.

#### 2.3.2.5 Top height of the plant $d + z_0$

The location of the plant layer is either treated at the top height of the plant or at the height  $d + z_0$ , in which  $d$  is the displacement height and  $z_0$  is crop roughness length for momentum (m),  $d$  is the distance between the plant layer and  $z_0$ .  $d$  and  $z_0$  are related to crop height  $h_c$  for the fully developed crop (i.e.,  $LAI \geq 4.0$ ) through the following expressions (Monteith, 1990):

$$d = 0.63h_c, \quad z_0 = 0.13h_c \quad (36)$$

with  $h_c$  varying with the growth of wheat where  $LAI$  is the projected area of leaf per unit ground area (leaf area index) (dimensionless).

#### 2.3.2.6 Aerodynamic resistances $r_a^a$ and $r_m^p$

The aerodynamic resistance varies according to the atmosphere situations, such as neutral, stable, and unstable (Camillo and Gurney, 1986). Herein, a neutral atmosphere is considered for  $r_a^a$  and  $r_a^s$  according to the local meteorological condition. Thus, when the “big leaf” (Alves et al. 1998) is considered to be at the  $d + z_0$  level, the formulations are described as follows (Shuttleworth and Wallace, 1985):

$$\left. \begin{aligned} r_a^a &= \frac{1}{4} LAI r_a^a(\beta) + \frac{1}{4} (4 - LAI) r_a^a(0) \\ r_a^s &= \frac{1}{4} LAI r_a^s(\beta) + \frac{1}{4} (4 - LAI) r_a^s(0) \end{aligned} \right\} \quad 0 \leq LAI \leq 4.0 \quad (37)$$

$$\left. \begin{aligned} r_a^a &= r_a^a(\beta) \\ r_a^s &= r_a^s(\beta) \end{aligned} \right\} \quad LAI > 4.0 \quad (38)$$

where  $LAI$  is fitted into an empirical formula against time via developing the relationship between  $LAI$  and the growth stage of wheat;  $r_a^a(\beta)$  and  $r_a^s(\beta)$  are the values for plant with complete canopy cover whilst  $r_a^a(0)$  and  $r_a^s(0)$  are the corresponding values with bare soil ( $\text{s m}^{-1}$ ), respectively. Their formulations are as follows:

$$r_a^a(\beta) = \frac{1}{ku_*} \left[ \ln\left(\frac{h_r - d}{h_c - d}\right) + \frac{h_c}{\eta(h_c - d)} \left[ \exp\left[\eta\left(1 - \frac{d + z_0}{h_c}\right)\right] - 1 \right] \right] \quad (39)$$

$$r_a^s(\beta) = \frac{1}{ku_*} \frac{h_c}{\eta(h_c - d)} [\exp \eta - \exp[\eta(1 - \frac{d + z_0}{h_c})]] \quad (40)$$

$$r_a^s(0) = \ln(h_r / z_0') \ln[(d + z_0) / z_0'] / k^2 u \quad (41)$$

$$r_a^a(0) = \ln(h_r / z_0') / ku - r_a^s(0) \quad (42)$$

in which  $\eta$  is an extinction coefficient with value of 2.5 for this specified crop (Monteith, 1990);  $z_0'$  is effective roughness length for momentum of the soil (equals 0.01m for bare soil),  $k$  is von Karman's constant (dimensionless),  $u_*$  is the friction velocity ( $\text{m s}^{-1}$ ),  $u$  is the wind speed at the reference height ( $\text{m s}^{-1}$ ).  $u_*$  is expressed as follows:

$$u_* = \frac{ku}{\ln[(h_r - d) / z_0]} \quad (43)$$

The difference between  $r_a^s$  and  $r_m^p$  is that the lower boundary integral of the former is the soil surface (Shuttleworth and Wallace 1985) whilst that of the latter is at the mulch surface. It can be assumed that the roughness length of transparent polyethylene is 0. After performing integration with the lower boundary  $h_m$  (the distance between soil layer and mulch layer),  $r_m^p(\beta)$ ,  $r_m^p(0)$ , and  $r_a^a(0)$  are expressed as follows:

$$r_m^p(\beta) = \frac{1}{ku_*} \frac{h_c}{\eta(h_c - d)} [\exp[\eta(1 - \frac{h_m}{h_c})] - \exp[\eta(1 - \frac{d + z_0}{h_c})]] \quad (44)$$

$$r_m^p(0) = \ln(h_r / h_m) \ln[(d + z_0) / h_m] / k^2 u \quad (45)$$

$$r_a^a(0) = \ln(h_r / h_m) / ku - r_m^p(0) \quad (46)$$

Thus  $r_a^a$  and  $r_m^p$  in the SMPAC system become:

$$\left. \begin{aligned} r_a^a &= \frac{1}{4} LAI r_a^a(\beta) + \frac{1}{4} (4 - LAI) r_a^a(0) \\ r_m^p &= \frac{1}{4} LAI r_m^p(\beta) + \frac{1}{4} (4 - LAI) r_m^p(0) \end{aligned} \right\} \quad 0 \leq LAI \leq 4.0 \quad (47)$$

$$\left. \begin{aligned} r_a^a &= r_a^a(\beta) \\ r_m^p &= r_m^p(\beta) \end{aligned} \right\} \quad LAI > 4.0 \quad (48)$$

### 2.3.2.7 Aerodynamic boundary layer resistance $r_a^c$

In terms of boundary layer theory, the resistance  $r_a^c$  or the conductivity of latent heat  $g_b$  ( $\text{m s}^{-1}$ ) depends on wind velocity as follows (Lhomme, 1988):

$$g_b(z) = \frac{1}{r_a^c(z)} = a(u(z) / w)^{0.5} \quad (49)$$

where  $w$  is the leaf width (m);  $a$  is assigned the value  $0.01 \text{ (ms}^{-0.5}\text{)}$ ;  $u(z)$  is the wind speed at the height  $z$  within the canopy layer. For the whole canopy,  $\overline{g_b}$ , the average conductivity per unit of leaf area index, is calculated by Choudhury et al. (1988) as follows:

$$\overline{g_b} = \frac{2a}{\eta} \left(\frac{u_c}{w}\right)^{0.5} [1 - \exp(-\frac{\eta}{2})] \quad (50)$$

where,  $u_c$  is the wind speed at the top of canopy layer. Thus, the aerodynamic boundary layer resistance  $r_a^c$  for the plant layer is obtained by the following expression:

$$r_a^c = \frac{1}{LAI g_b} \quad (51)$$

### 2.3.2.8 Total stomatal resistance $r_a^p$

According to Lu (1992),  $r_a^p$  is related to the net radiation  $R_n$  ( $\text{W m}^{-2}$ ), vapor pressure deficit  $D$  at reference height (mba) ( $D = e_{sat}(T_a) - e_a$ , where  $e_{sat}(T_a)$  is the saturation vapor pressure corresponding to the air temperature  $T_a$ ),  $LAI$ , and leaf water potential  $\psi_l$  (cm):

$$r_a^p = 100.0 / [(2.867LAI + 0.0277(1 - e^{\eta LAI})R_n / k)(1 - 0.0254D) / (1 + (-\psi_l / 31529)^{4.58})] \quad (52)$$

in which  $\eta$  is the extinction coefficient of  $R_n$  within the canopy layer (dimensionless).

### 2.3.2.9 Resistance to convective heat transfer $r_s^m$

Although the distance between the soil and mulch is small, air still acts as a medium in transferring the sensible heat, which is treated as free convection. The resistance  $r_s^m$  can be formulated as follows:

$$r_s^m = \frac{\rho_a c_p d_l}{k_T Nu} \quad (53)$$

in which the characteristic length  $d_l$  (m) is the distance between mulch and soil surface. Herein it is set to be 0.125;  $k_T$  is air heat conductivity ( $\text{W m}^{-1} \text{ }^\circ\text{C}^{-1}$ );  $Nu$  is Nusselt number.

### 2.3.2.10 Other parameters in energy balance equation

Since many parameters in energy balance equations are varying with the growth of wheat, empirical equations are derived based on three-month field observations from March to June:

$$r_{pg} = -8 \times 10^{-5} i_d^2 + 0.0079 i_d + 0.0828 \quad (54)$$

$$\eta = -3 \times 10^{-6} i_d^3 + 0.0002 i_d^2 + 0.0148 i_d \quad (55)$$

$$r_{mg} = -0.0003 i_d^2 + 0.0175 i_d + 0.0398 \quad (56)$$

in which  $i_d$  is time (days) beginning on 15<sup>th</sup> March. Moreover, other parameters are determined from literature (Mahrer et al., 1984; Chung and Horton, 1987; Kluitenberg, 1994; Flerchinger et al., 2003):  $t_{pg} = 1 - \eta - r_{pg}$ ;  $t_{pl} = t_{pg}$ ,  $t_{mg} = 0.85$ ;  $r_{sg} = 0.20$ ;  $r_{ml} = 0.12$ ;  $t_{ml} = 0.78$ ;  $\varepsilon_p = \eta$ ;  $\varepsilon_s = 0.90 + 0.18\theta_l$ ;  $a_{pl} = 1 - r_{pl} - t_{pl}$ ;  $a_{pg} = \eta$ ;  $a_{mg} = 1 - t_{mg} - r_{mg}$ ; and  $a_{ml} = 1 - t_{ml} - r_{ml}$ .

### 2.3.2.11 Global radiation $R_g$

The global radiation is expressed as a function of time (Chung and Horton, 1987)

$$R_g = (\pi / 2) DR / DL \sin[(t - SN + DL / 2)\pi / DL] \quad (57)$$

where  $DR$  is daily global radiation ( $\text{J m}^{-2}$ ),  $t$  is the time of a day (s),  $SN$  is solar noon (s), and  $DL$  is daylength (s). In the application, it is found that the computational error for  $R_g$  is very significant if  $DR$  cannot be measured precisely. Thus, in this study, an alternative approach is adopted, which is based on the sinusoidal distribution for  $R_g$  in a day when the weather situation is stable. This condition is justified in this region during the wheat growth period. An empirical equation for  $R_g$  is described as follows:

$$R_g = A_0 \sin(\omega t + \psi) \quad (58)$$

in which  $A_0$  is the amplitude of the function ( $\text{W m}^{-2}$ ), which is value of  $R_g$  at 12:00; the angular frequency  $\omega$  is equal to  $\pi / 12$  ( $\text{s}^{-1}$ ); and the phase angle  $\psi$  is  $-\pi / 2$  (radian).

### 2.3.2.12 Air temperature $T_a$ , dew-point temperature $T_d$ , and water vapor temperature $T_w$

The temporal variation of temperatures  $T_a$ ,  $T_d$ , and  $T_w$  are represented as follows:

$$T_a(t) = T_{av} + T_{a0} \sin\left[\frac{\pi(t/3600 - 10)}{12}\right] \quad (59)$$

$$T_w(t) = T_{wv} + T_{w0} \sin\left[\frac{\pi(t/3600 - 10)}{12}\right] \quad (60)$$

$$T_d(t) = T_{dv} + T_{d0} \sin\left[\frac{\pi(t/3600 - 10)}{12}\right] \quad (61)$$

where  $T_{av}$ ,  $T_{dv}$ , and  $T_{wv}$  are the daily average of  $T_a$ ,  $T_d$ , and  $T_w$ , respectively,  $T_{a0}$ ,  $T_{d0}$ , and  $T_{w0}$  represent amplitudes, and  $t$  is the time of a day beginning from midnight (s).

### 2.3.2.13 Saturated vapor pressure $e_{sat}(T_i)$ at temperature $T_i$

The following equations (De Silans et al., 1989) are used to compute the saturated vapor pressure at temperature  $T_i$ :

$$e_{sat}(T_i) = 6.1078 \times 10^{7.63T_i / (241.9 + T_i)} \quad T_i > 0 \quad (62)$$

$$e_{sat}(T_i) = 6.1078 \times 10^{9.5T_i / (265.5 + T_i)} \quad T_i \leq 0 \quad (63)$$

## 2.4 Modelling strategy

### 2.4.1 Calibration

The alternating direction implicit finite difference method is used to discretize the governing equations (Mohamed, 2003). The energy balance equations are solved by using an iterative Newton-Raphson technique, from which  $T_p$ ,  $T_l$ ,  $T_m$ , and  $T_s$  can be obtained.  $S_r$  and  $G$  in the governing equations can then be computed after having determined  $T_l$  and  $T_s$ . Before the model can be used to predict, it has to be calibrated. The parameters  $P$ ,  $Q$ ,  $b_1$ ,  $b_2$  and  $b_3$ , which are used to compute hydraulic conductivity and thermal conductivity of the cropland, are determined in the calibration process. It is a tedious job to determine these parameters manually. Hence a genetic algorithm with global search ability is employed to optimize them in this study. The optimized parameters are listed in Table 1.

The incremental time step  $\Delta t$  and spatial step  $\Delta z$  adopted are 200 s and 0.02 m, respectively. Moreover, tolerances  $\varepsilon_T$  and  $\varepsilon_h$  of temperature  $T$  and matric potential  $h$  in the soil profile are 0.1 °C and 0.1 cmH<sub>2</sub>O respectively at the steady state whilst the tolerant differential errors of  $h$  and  $T$  between any two consecutive computational times are 0.01 °C and 0.01 cmH<sub>2</sub>O respectively. These are measures set to prevent the occurrence of any undesirable numerical instability during the modeling process. In this study, observed data on March 15 are employed to calibrate this model, and the root mean square error (RMSE) and mean error (ME) are adopted as the evaluation criteria for model performance. which are adopted in percentages as below:

$$RMSE = \sqrt{\frac{\sum_{i=1}^p \left[ \frac{(X_o)_i - (X_s)_i}{(X_s)_i} \right]^2}{p}} \times 100\% \quad (64)$$

$$ME = \frac{\sum_{i=1}^p \left[ \frac{(X_o)_i - (X_s)_i}{(X_s)_i} \right]}{p} \times 100\% \quad (65)$$

where subscripts  $o$  and  $s$  denote the observed and simulated values, respectively;  $p$  = total number of observed sites in the same soil profile ( $p=7$  for  $T$  and  $p=8$  for  $\theta_l$ ). In view of the rather large variations in soil temperature and water content during the wheat growth, criteria on relative errors are often better than absolute errors. The calibration process is carried out so as to minimize both RMSE and MW.

#### 2.4.2 Validation/Prediction

Based on calibrated model, profiles of soil temperature and water content and other parameters can be simulated. Simulations are carried out in three phases, namely, phase one (reviving to elongation stage, from March 20 to April 15), phase two (elongation to heading stage, from April 25 to May 10), and phase three (stage of yellow ripeness, from May 24 to June 10).

### 3. Results and discussion

#### 3.1 Modelling results

Fig. 2, Fig. 3, and Fig.4 show the simulated and observed profiles of soil water content  $\theta_l$  and temperature  $T$  in phases one, two, and three, respectively, with the corresponding error values listed in Table 2. It can be seen that good agreements exist for both  $\theta_l$  and  $T$ . The results in Table 2 indicate that the relative errors of water content  $\theta_l$  are all less than 30% whilst most errors of temperature  $T$  are less than 31.5%, except the temperature on March 25. As moisture dynamics and temperature dynamics are coupled, the excessively high error on March 25 is counterbalanced by an opposite error on  $\theta_l$ . In addition, in phases one and two, the error fluctuations about  $\theta_l$  and  $T$  are small since values of ME and MRSE are close to each other. However, in phase three, the error fluctuations about  $T$  are small whereas those for  $\theta_l$  are quite different.

Comparisons are also made between simulated and observed values of mulch temperature  $T_m$  and soil surface temperature  $T_s$ . The simulated  $T_m$  and  $T_s$  versus time are depicted in Fig. 5 and Fig. 6, respectively. Their relative errors in the three phases are listed in Table 3, which are in the range from 20% to 30% in general. For  $T_s$ , the relative error in phase one, which is 51.3%, is higher than the other two phase.

The simulated values of the plant layer temperature  $T_p$  and the leaf temperature  $T_l$  are depicted in Fig.7. Owing to the lack of observed values, similar comparisons between simulation and observation data cannot be made. Nevertheless, it can be observed that their values are within reasonable temperature range when the experiments took place.

The comparison of transpiration between simulated and observed data is shown in Table 4. The error in phase one is particularly large. Although the mean errors are small in the latter two phases, the fluctuations of errors are obvious because there is a large difference between RMSE and ME.

#### 3.2 Discussions

Although very complicated physical processes are involved in this prototype SMPAC model, some possible reasons can be suggested for the variation of errors. It is found that the model performs particularly well when water content  $\theta_l$  of soil profile is relatively high, but less so when  $\theta_l$  is low. A possible reason for this is that the effect of the vapor generally increases when  $\theta_l$  is low. In the model, the vapor may not be simulated with sufficient accuracy, thus leading to larger errors when its effect becomes significant. In the three phases, the model shows very good performance on temperature  $T$  of soil profile except on March 25 in comparison with water content  $\theta_l$  of soil profile. The relative errors of soil surface temperature  $T_s$  can be grouped together with the relative errors of  $T$  since  $T_s$  is the value of  $T$  at zero depth in the soil profile. Therefore, a possible reason for their errors is the measurement inaccuracy of  $T_s$  that may be attributable to thermometer or observer. Of course, it is also difficult to get a good measurement of  $T_m$  because of direct radiation at the mulch level. In comparison with  $T_s$ , this model performs better on temperature  $T_m$  of mulch layer.

In addition, when compared with the observed data in Table 4, the simulated transpiration

amounts tend to be a bit overestimated particularly in the phase one. A possible reason is that owing to the omission of evaporation from soil surface and the conservation of the mass water balance in this system, it leads to increase in the simulated transpiration amount. The larger error in the first phase than the latter phases may be explained by its higher soil evaporation due to a smaller LAI. On the other hand, a larger LAI will cause more transpiration but less soil evaporation.

### 3.3 Sensitivity analysis

Many parameters are concerned with this model. Therefore, a sensitivity analysis would help identifying the main processes or parameters responsible for the observed discrepancies.

Although some characteristic parameters of the soil are calibrated, the model performance is strongly related to some energy parameters. Two parameters, namely, emissivity of the plant layer  $\varepsilon_p$  and extinction coefficient  $\eta$ , are studied for their sensitivity. The emissivity of the plant layer is set to the value of  $\varepsilon_p$  (0.64 for  $\varepsilon_p$  in this analysis),  $1.25 * \varepsilon_p$ ,  $0.75 * \varepsilon_p$ , and  $0.5 * \varepsilon_p$ , respectively. Similarly, the extinction coefficient is set to the observed value ( $\eta$ ),  $1.25 * \eta$ ,  $0.85 * \eta$ ,  $0.75 * \eta$ ,  $0.5 * \eta$ , and  $0.25 * \eta$ , respectively.

Table 5 shows that the corresponding variations for transpiration are (27%, -75%) and (-35%, 101%) when  $\eta$  and  $\varepsilon_p$  respectively vary from (125%, 25%) and (125%, 50%). Therefore,  $\eta$  is positively correlated to the transpiration whereas  $\varepsilon_p$  is negatively correlated to the transpiration. Fig 8 and Fig.9 show that soil temperatures are more sensitive to  $\eta$  and  $\varepsilon_p$  than water contents. Moreover, both soil temperatures and water contents are more sensitive to  $\varepsilon_p$  than  $\eta$ . It can be observed that lesser  $\varepsilon_p$  is related to lesser water content (i.e. larger transpiration amount), which is consistent to the result in the sensitivity analysis of transpiration. However, the relationship between  $\eta$  and water contents is not obvious in comparison with the sensitivity analysis of transpiration. Furthermore, the results also show that larger  $\varepsilon_p$  is related to larger soil temperature whilst  $\eta$  has an opposite effect on the soil temperature. Therefore, an appropriate choice of values on energy parameters may be a significant factor in improving the model performance.

## 4. Conclusions

In this paper, a coupled water and heat transport model is developed to represent physical processes in a SMPAC system. The model calibrated by the observed data on March 15 is applied to three distinct phases of the growth period of the winter wheat, namely, reviving to elongation stage, elongation to heading stage, and stage of yellow ripeness. The agreement is good between simulated and observed values for soil profile temperature and soil water content in all three phases, in particular under high soil water content. The model shows slightly better simulation performance on the mulch layer temperature than on soil surface temperature. Performances on simulations of transpiration amounts in the later two growing phases are slightly better than that in the first phase. The results of the sensitivity analysis of some key model parameters demonstrate that an appropriate choice of values on energy parameters may be a significant factor in improving the model performance. Since complicated physical processes have been captured into this reasonably accurate four-layered system, it can be adopted to determine the most appropriate irrigation schedule for similar croplands.

## References

- Alves, I., Perrier, A., and Pereira, L.S. (1998). "Aerodynamic and surface resistances of complete cover crops: how good is the 'big leaf'?" *Transactions of the ASAE*, 41(2), 345-351.
- Bolger, T.P., Upchurch, D. R., and McMichael, B. L. (1992). "Temperature effects on cotton root

hydraulic conductance.” *Environmental and Experimental Botany*, 32(1), 49-54.

Camillo, P.J., and Gurney, R.J. (1986). “A resistance parameter for bare-soil evaporation models.” *Soil Science*, 141(2), 95-105.

Chung, S.O., and Horton R. (1987). “Soil heat and water flow with a partial surface mulch.” *Water Resources Research*, 23(12), 2175-2186.

De Silans, A.P, Bruckler, L., Thony, J.L., and Vauclin, M. (1989). “Numerical modeling of coupled heat and water flows during drying in a stratified bare soil — Comparison with field observations.” *Journal of Hydrology*, 105(1-2), 109-138.

de Vries, D.A. (1958). “Simultaneous transfer of heat and moisture in porous media.” Transactions, American Geophysical Union, Vol. 39, No. 5, 909-916.

Findeling, A., Chanzy, A., De Louvigny, N. (2003a). “Modeling water and heat flows through a mulch allowing for radiative and long-distance convective exchanges in the mulch.” *Water Resources Research*, 39 (9), 1244.

Findeling, A, Ruy, S, and Scopel, E. (2003b). “Modeling the effects of a partial residue mulch on runoff using a physically based approach.” *Journal of Hydrology*, 275(1-2), 49-66.

Flerchinger, G.N., Sauer, T.J., Aiken, R.A. (2003). “Effects of crop residue cover and architecture on heat and water transfer at the soil surface.” *Geoderma*, 116(1-2), 217-233.

Gonzalez-Sosa, E., Braud, I., Thony, J.L., Vauclin, M., Bessemoulin, P. and Calvet, J.C. (1999). “Modelling heat and water exchanges of fallow land covered with plant-residue mulch.” *Agricultural and Forest Meteorology*, 97(3), 151-169.

Gonzalez-Sosa, E., Braud, I., Thony, J.L., Vauclin, M. and Calvet, J.C. (2001). “Heat and water exchanges of fallow land covered with a plant-residue mulch layer: a modeling study using the three year murex data set.” *Journal of Hydrology*, 244(3-4), 119-136.

Ham, J.M., and Kluitenberg, G.J. (1994). “Modeling the effect of mulch optical properties and mulch-soil contact resistance on soil heating under plastic mulch culture.” *Agricultural and Forest Meteorology*, 71(3-4), 403-424.

Huang, J.S., and Shen, R.K. (1999). “Analysis of crop evapotranspiration under transparent polyethylene mulch.” 17<sup>th</sup> ICID Congress on Irrigation and Drainage, Vol. 1A, 327-338.

Kim, J., Verma, S.B., and Rosenberg, N.J. (1989). “Energy balance and water use of cereal crops.” *Agricultural and Forest Meteorology*, 48(1-2), 135-147.

Lafleur, P.M.. (1992). “Energy balance and evapotranspiration from a sub-arctic forest.” *Agricultural and Forest Meteorology*, 58(3-4), 163-175.

Lhomme, J.P. (1988). “A generalized combination equation derived from a multi-layer micrometeorological model.” *Boundary-Layer Meteorology*, 45, 103-115.

Lu, Z.M. (1992). “Dynamic simulation and experiment studies on water flow in Soil-Plant-Atmosphere Continuum system: II. Determining water resistances in SPAC system.” Studies on relation between plant and water, Chinese Science and Technology Press (in Chinese).

Luo, Y., Loomis, R.S., and Hsiao, T.C. (1992). “Simulation of soil temperature in crops.” *Agricultural and Forest Meteorology*, 61(1-2), 23-38.

Mahrer, Y., Naot, O., Rawitz, E., and Katan, J. (1984). “Temperature and moisture regimes in soils mulched with transparent polyethylene.” *Soil Science Society of America Journal*, 48(2), 362-367.

McGinn, S.M., and King, K.M. (1990). “Simultaneous measurements of heat, water vapor and CO<sub>2</sub> fluxes above alfalfa and maize.” *Agricultural and Forest Meteorology*, 49(4), 331-349.

Milly, P.C.D. (1984). “A simulation analysis of thermal effects on evaporation from soil.” *Water Resources Research*, 20(8), 1087-1098.

Milly, P.C.D., and Eagleson, P.S. (1980). “The coupled transport of water and heat in a vertical soil column under atmospheric excitation.” Tech. Rep. 258, R.M. Parsons Lab., Dep. Of Civil Egn., Mass. Inst, of Technol., Cambridge.

Mohamed, I.O. (2003). “Computer simulation of food sterilization using an alternating direction

implicit finite difference method.” *Journal of Food Engineering*, 60(3), 301-306.

Monteith, J.L. (1990). *Principles of Environmental Physics*. Edward Arnold, London.

Shuttleworth, W.J., and Wallace, J.S. (1985). “Evaporation from sparse crops - an energy combination theory.” *Quarterly journal of the Royal Meteorological Society*, 111(469), 839-855.

Van Bavel, C.H.M., and Hillel, D.I. (1976). “Calculating potential and actual evaporation from a bare soil surface by simulation of concurrent flow of water and heat.” *Agricultural Meteorology*, Vol. 17, No. 6, 453-476.

Van Genuchten, M. TH. (1980). “A closed-form equation for predicting the hydraulic conductivity of unsaturated soils.” *Soil Science Society of America Journal*, 44(5), 892-898.

Table 1 Characteristic parameters of the soil

Depth (cm)	$\theta_s$ ( $\text{m}^{-3} \text{m}^{-3}$ )	$\theta_r$ ( $\text{m}^{-3} \text{m}^{-3}$ )	$\alpha$ ( $\text{m}^{-1}$ )	$n$ (dimension- less)	$P$ ( $\text{s}^{-1}$ )	$Q$ (dimension -less)	$b_1$ ( $\text{Js}^{-1}\text{m}^{-10}\text{C}^{-1}$ )	$b_2$ ( $\text{Js}^{-1}\text{m}^{-10}\text{C}^{-1}$ )	$b_3$ ( $\text{Js}^{-1}\text{m}^{-10}\text{C}^{-1}$ )
0-70 (silt loam)	0.42	0.12	1.20	2.5	0.01467	-2.790	0.208	0.336	1.312
70-100 (sand)	0.39	0.04	1.23	1.68	0.00542	-3.050	0.195	-2.058	4.199

Table 2 Error results (%) between simulated and observed values of soil water content and temperature from 20 March to 5 June

		20 March	25 March	30 March	05 April	10 April	15 April			
Water content $\theta_l$ of soil profile	ME	11.6	10.8	12.4	21.0	17.8	12.4			
	MRSE	13.0	12.2	14.8	22.7	24.1	15.7			
Temperature $T$ of soil profile	ME	10.7	44.7	14.3	6.3	4.2	7.9			
	MRSE	11.2	47.0	15.6	10.8	4.8	9.3			
		25 April	30 April	5 May	10 May	24 May	30 May	5 June		
Water content $\theta_l$ of soil profile	ME	11.0	19.2	24.3	20.1	5.5	8.9	13.2		
	MRSE	15.8	23.6	29.2	29.4	20.6	24.0	20.9		
Temperature $T$ of soil profile	ME	5.8	19.2	25.3	22.1	0.9	19.2	8.8		
	MRSE	10.7	23.6	31.2	30.4	2.2	23.2	10.9		

Table 3 Error results (%) between simulated and observed values of mulch temperature  $T_m$  and soil surface temperature  $T_s$

		Phase 1 (20 March – 15 April)	Phase 2 (24 April – 10 May)	Phase 3 (24 May - 10 June)
Soil surface temperature $T_s$	ME	9.4	15.6	6.0
	MRSE	51.1	29.1	14.7
Mulch temperature $T_m$	ME	8.5	19.6	1.7
	MRSE	35.3	30.6	13.4

Table 4 Error results (%) between simulated and observed values of plant transpiration

	Average transpiration (mm/d)		RMSE	ME
Phase 1 (20 March – 15 April)	Simulated	4.35	57.6	39.7
	Observed	1.80		
Phase 2 (24 April – 10 May)	Simulated	5.71	44.5	13.5
	Observed	3.62		
Phase 3 (24 May - 10 June)	Simulated	4.79	50.6	6.2
	Observed	3.61		

Table 5 Variation of the simulated transpiration in sensitivity analysis

Extinction coefficient $\eta$	$1.25 * \eta$	Reference $\eta$ (observation)	$0.85 * \eta$	$0.75 * \eta$	$0.5 * \eta$	$0.25 * \eta$
Simulated transpiration amount (mm/d)	5.99	4.73	4.08	3.13	2.15	1.18
Emissivity of the plant layer $\varepsilon_p$	$1.25 * \varepsilon_p$	Reference $\varepsilon_p$ (0.64)		$0.75 * \varepsilon_p$	$0.5 * \varepsilon_p$	
Simulated transpiration amount (mm/d)	4.08	6.31		9.42	12.71	

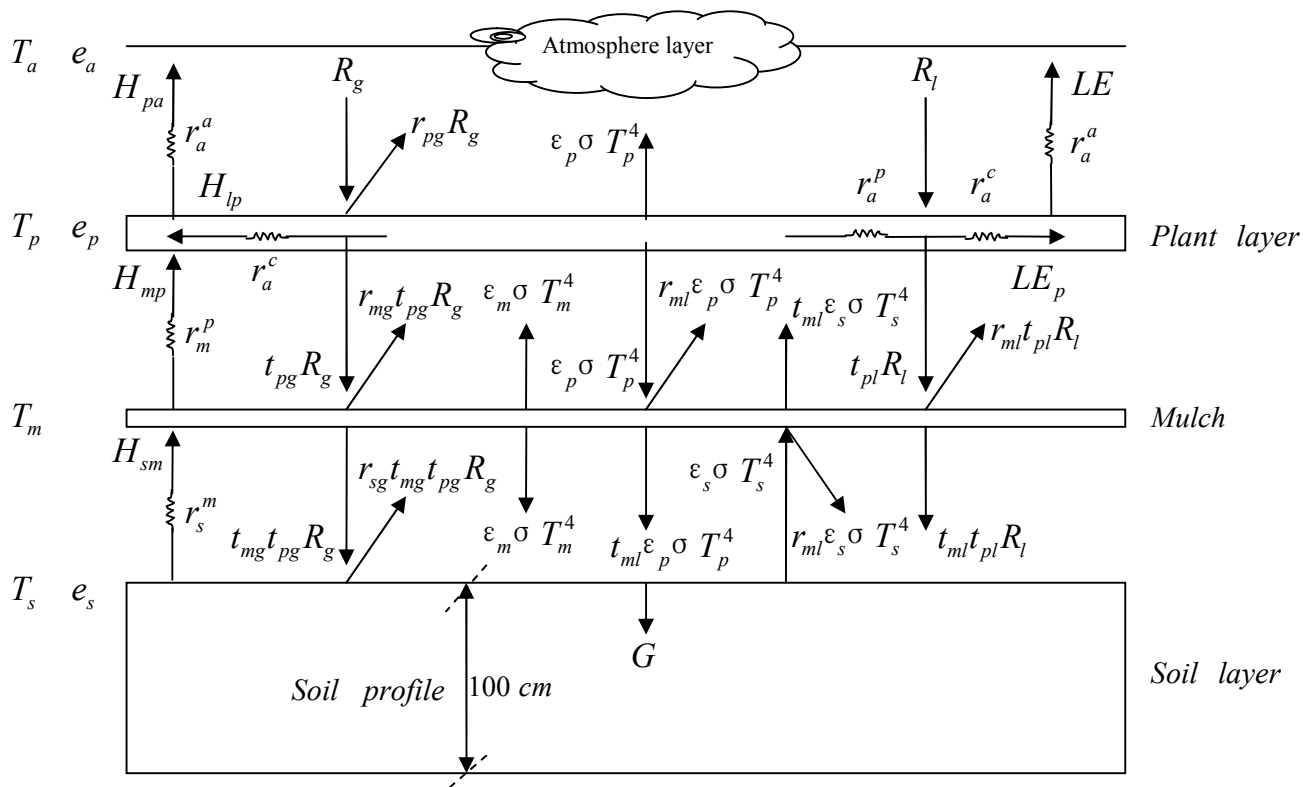


Fig.1 Schematic diagram of the SMPAC system

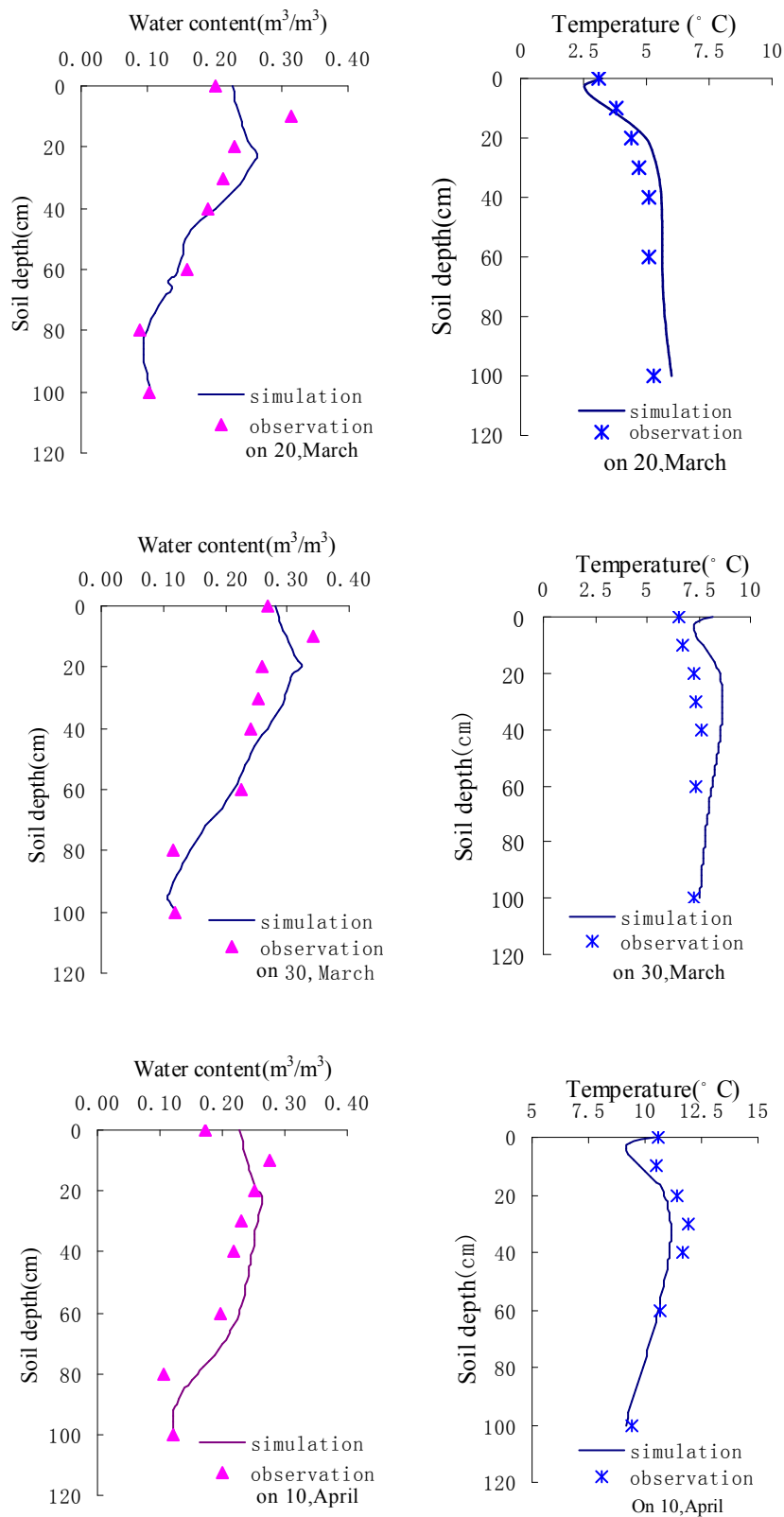


Fig.2 Comparison between simulated and observed values of  $\theta_i$  and  $T$  from 20 March to 15 April

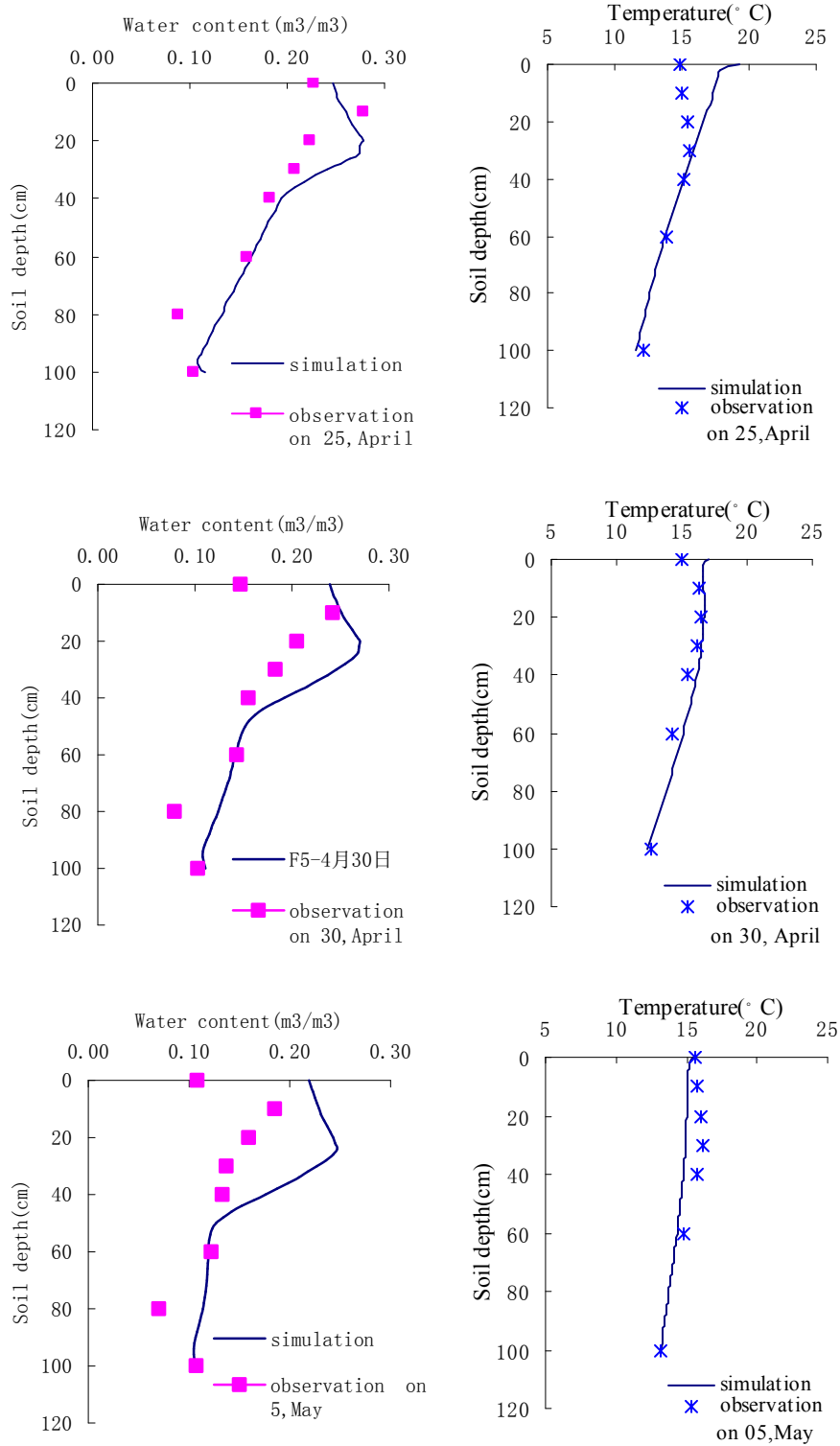


Fig.3 Comparison between simulated and observed values of  $\theta_l$  and  $T$  from 25 April to 10 May

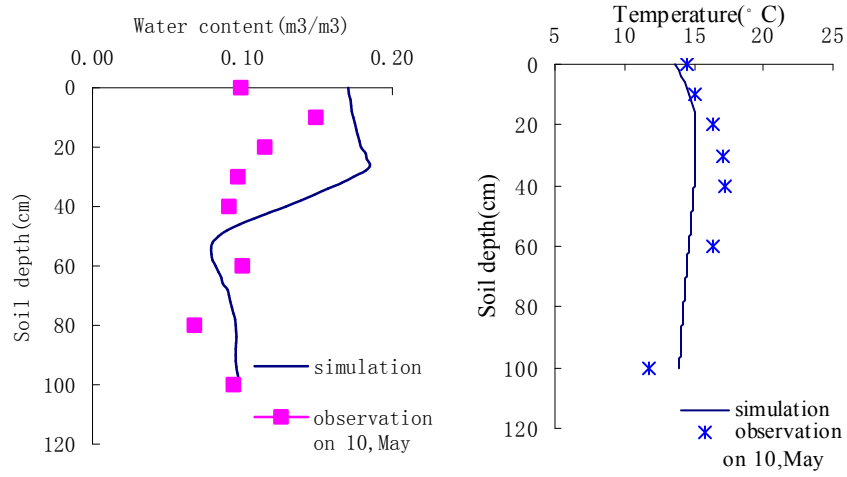


Fig.3 Comparison between simulated and observed values of  $\theta_l$  and  $T$  from 25 April to 10 May  
(cont'n)

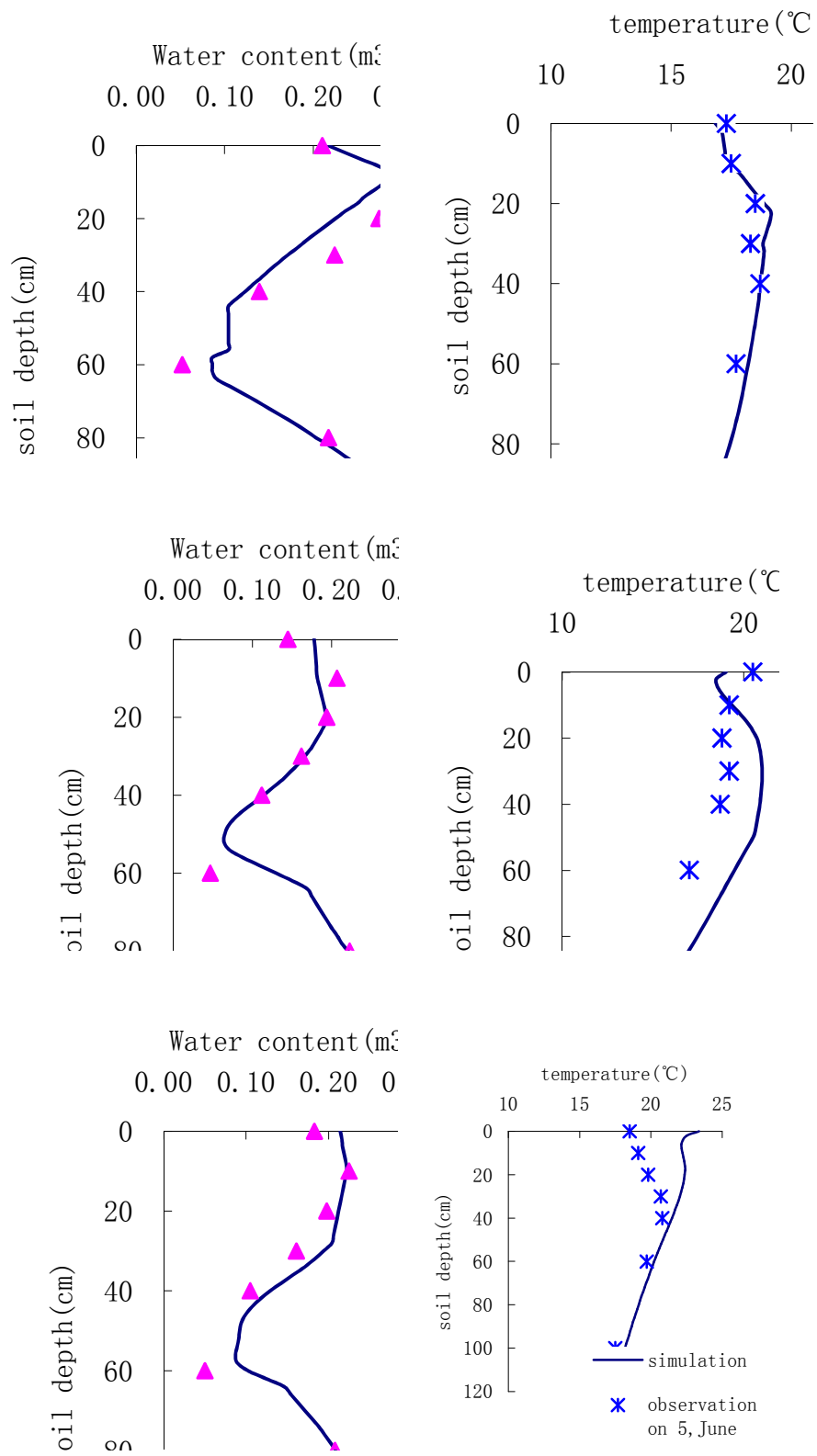


Fig.4 Comparison between simulated and observed values of  $\theta_t$  and  $T$  from May 24 to June 10

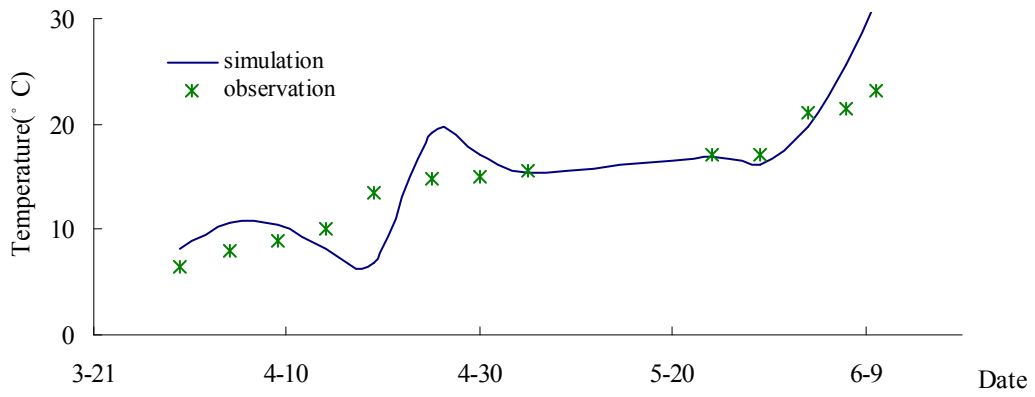


Fig.5 Comparison between simulated and observed values of  $T_m$  versus time

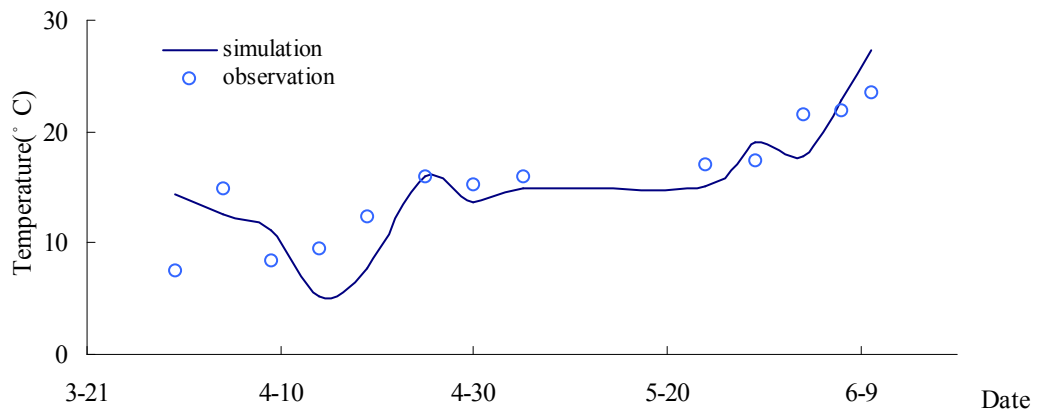


Fig. 6 Comparison between simulated and observed values of  $T_s$  versus time

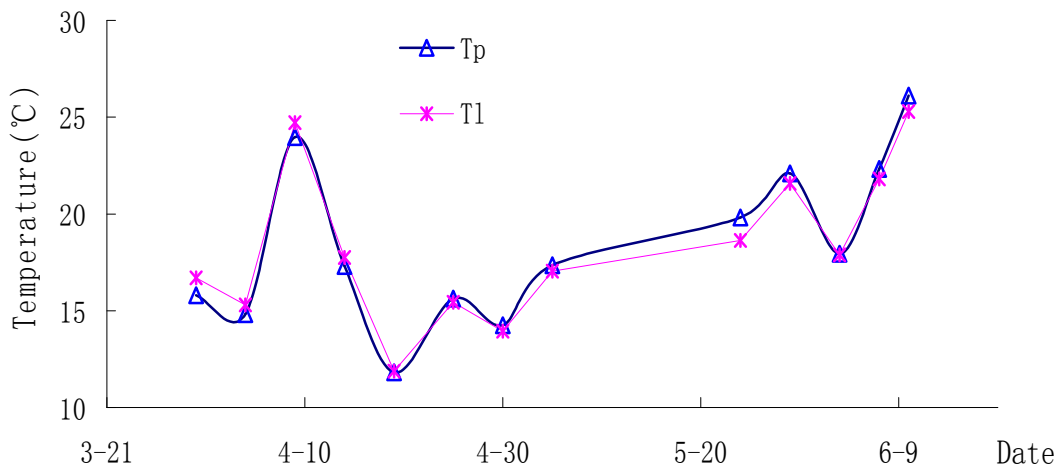


Fig. 7 Simulated values of temperatures  $T_p$  and  $T_l$  versus time

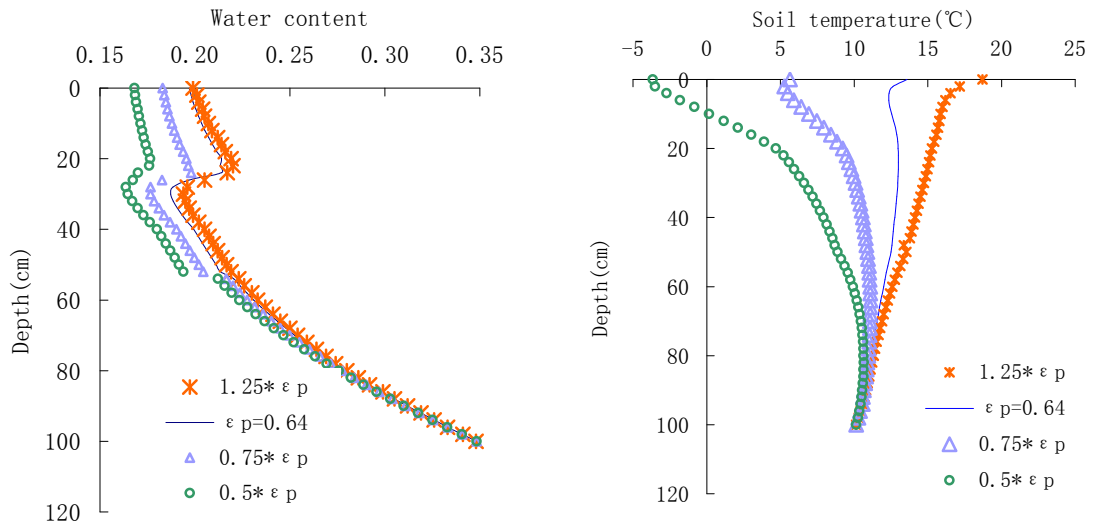


Fig. 8 Variation of soil temperatures and water contents for sensitivity analysis of emissivity  $\epsilon_p$

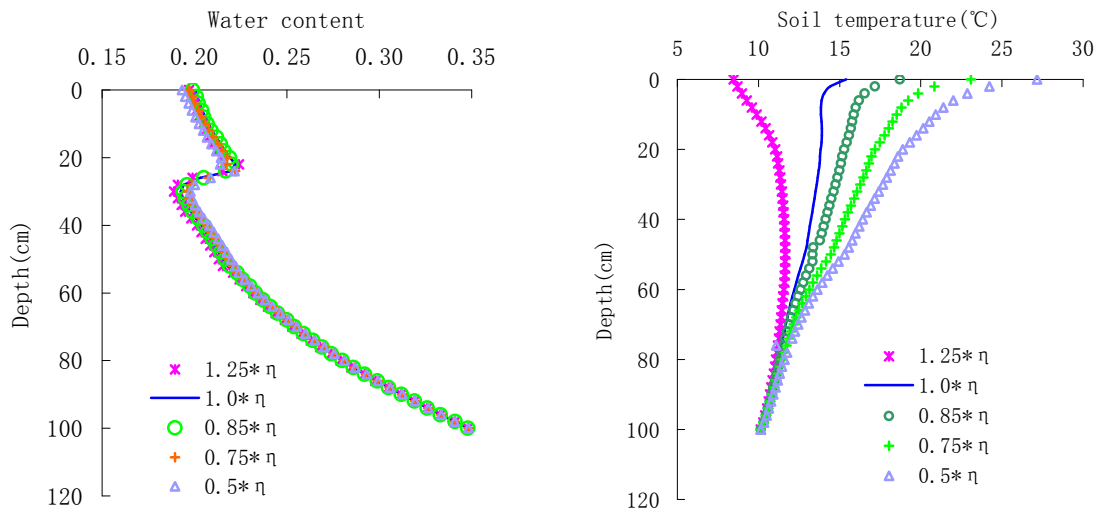


Fig. 9 Variation of soil temperatures and water contents for sensitivity analysis of extinction coefficient  $\eta$